

Quantum Adiabatic Brachistochrone

A. T. Rezakhani,¹ W.-J. Kuo,¹ A. Hamma,² D. A. Lidar,¹ and P. Zanardi¹

¹*Departments of Chemistry, Electrical Engineering, and Physics, and Center for Quantum Information Science & Technology, University of Southern California, Los Angeles, California 90089, USA*

²*Perimeter Institute for Theoretical Physics, 31 Caroline Street North, N2L 2Y5, Waterloo, Ontario, Canada*

(Received 14 May 2009; published 21 August 2009)

We formulate a time-optimal approach to adiabatic quantum computation (AQC). A corresponding natural Riemannian metric is also derived, through which AQC can be understood as the problem of finding a geodesic on the manifold of control parameters. This geometrization of AQC is demonstrated through two examples, where we show that it leads to improved performance of AQC, and sheds light on the roles of entanglement and curvature of the control manifold in algorithmic performance.

DOI: [10.1103/PhysRevLett.103.080502](https://doi.org/10.1103/PhysRevLett.103.080502)

PACS numbers: 03.67.Lx, 02.30.Xx, 02.30.Yy, 02.40.-k

Introduction.—Quantum computation is most commonly formulated in the language of the “circuit model” [1]. The problem of finding optimal quantum circuits—which minimize the number of gates used—was recently addressed in an elegant differential-geometric framework, wherein the minimum number of elementary gates for construction of a general n -qubit unitary U can be found by traversing the geodesic connecting the identity $\mathbb{1}$ to U over the $SU(2^n)$ manifold [2]. This approach is appealing since it allows for the application of powerful tools and techniques from variational calculus and differential geometry [3] to quantum computation. Adiabatic quantum computation (AQC) [4], on the other hand, is a very different approach which has recently attracted much attention due to its fundamental connection to quantum many-body systems, in particular, to quantum phase transitions (QPTs) [5]. The basic strategy of AQC is to solve computational problems based on adiabatic evolution. A quantum system is prepared in the ground state of an initial Hamiltonian $H(0) = H_I$. The system is then adiabatically driven to a final state, which is close to the ground state of a “problem Hamiltonian” $H(T) = H_P$. This final state corresponds to the solution of a hard problem, while a short time T corresponds to an efficient AQC strategy. Although AQC is equivalent in computational power to the circuit model [6], it is still relatively unexplored. Specifically, an optimal strategy for AQC, akin to what has been done for the circuit model [2], has not yet been formulated.

In this Letter we reformulate AQC as a variational problem and develop a time-optimal strategy—a “quantum adiabatic brachistochrone” (QAB)—for quantum algorithms [7]. Specifically, we devise a variational time-optimal strategy for obtaining an interpolating Hamiltonian $H(t)$ between H_I and H_P , which gives rise to the shortest time T while guaranteeing that the actual final state (the solution to the corresponding Schrödinger equation), is close to the desired final ground state. We go further and show that the QAB can be recast in a natural differential-geometric framework. We provide two examples which illustrate the advantage of this optimal approach.

Time-optimal AQC.—The adiabatic approximation, which underlies AQC, is often stated as follows [8]. Consider a system subjected to a time-dependent Hamiltonian $H(t)$, with a nondegenerate ground state $|\Phi_0(t)\rangle$ isolated by a nonvanishing gap $\Delta(t)$ from the first excited state $|\Phi_1(t)\rangle$. Let $D(t) \equiv |\langle \Phi_1(t) | \partial_t H(t) | \Phi_0(t) \rangle|$. Prepare the system in $|\psi(0)\rangle = |\Phi_0(0)\rangle$ and let it evolve according to the Schrödinger equation into the state $|\psi(T)\rangle$. Then, provided the time variation of the Hamiltonian is sufficiently slow, or T is sufficiently large, in that $\max_{t \in [0, T]} D(t) / \min_{t \in [0, T]} \Delta^2(t) \ll \epsilon$, the fidelity $F(T) \equiv |\langle \Phi_0(T) | \psi(T) \rangle|$ between the final ground state and the actual final state is high: $F \geq \sqrt{1 - \epsilon^2}$. However, it is well known that the latter condition is not always accurate [9], as recently verified experimentally [10]. Rigorous versions of the adiabatic approximation [11] typically involve $\|\partial_t H\|^2 / \Delta^3$ (with the norm being the maximum eigenvalue), or terms with different powers of $\|\partial_t H\|$ and Δ . As our approach is to use the adiabatic condition as a heuristic for finding optimal trajectories, the exact form of the adiabatic condition is in fact not essential: we shall judge success by the tradeoff between fidelity F and evolution time T . As we show below, this pragmatic approach also allows us to find time-optimal and geometric formulations of AQC.

The time dependence of Hamiltonians usually comes from a set of control parameters $\mathbf{x}(t) = (x^1(t), \dots, x^M(t))^T$ —e.g., electric or magnetic fields, laser beams, or any other experimental “knob”—varying over a parameter manifold \mathcal{M} , whence $H = H[\mathbf{x}(t)]$. Varying the Hamiltonian for a given interval $t \in [t_0, t_1]$ then translates geometrically into moving along a control curve (or path) $\mathbf{x}(t)$ in \mathcal{M} . We can reparametrize \mathcal{M} via a dimensionless “natural parameter” $s(t)$ [3], with $s(0) = 0$ and $s(T) = 1$ (e.g., the normalized length), where $v(t) \equiv ds/dt > 0$ characterizes the speed by which we move along $\mathbf{x}[s(t)] \in \mathcal{M}$. To make the adiabatic dynamics locally compatible with the geometric structure of \mathcal{M} , we modify the adiabatic condition into the following local form [12]:

$$\frac{v(s)\|\partial_s H(s)\|}{\Delta^2(s)} \ll \epsilon \quad \forall s \in [0, 1]. \quad (1)$$

To ensure analyticity and to enable a geometric treatment, hereafter the norm is the Hilbert-Schmidt (or Frobenius) norm, defined as $\|A\|_{\text{HS}} = \sqrt{\text{Tr}[A^\dagger A]}$. From the relation $T = \int_0^1 ds/v(s)$, we define the adiabatic time-functional

$$\mathcal{T}[\mathbf{x}(s)] = \int_0^1 \frac{ds}{v_{\text{ad}}[\dot{\mathbf{x}}(s), \mathbf{x}(s)]} \equiv \int_0^1 ds \mathcal{L}[\dot{\mathbf{x}}(s), \mathbf{x}(s)], \quad (2)$$

where $\dot{x} \equiv \partial_s x$. Inspired by the local condition (1), we choose the instantaneous ‘‘adiabatic speed’’ via the ansatz

$$v_{\text{ad}}(s) \equiv \epsilon \Delta^2(s) / \|\partial_s H(s)\|_{\text{HS}}, \quad (3)$$

and hence—using Einstein summation—the Lagrangian $\mathcal{L}[\dot{\mathbf{x}}(s), \mathbf{x}(s)] = \|\dot{x}^i \partial_i H[\mathbf{x}(s)]\|_{\text{HS}} / \epsilon \Delta^2[\mathbf{x}(s)]$, where $\partial_i \equiv \partial/\partial x^i$. This ansatz is sensible, in that adiabaticity is hindered when the gap closes, while it is favored when the variation of the Hamiltonian is slow. To simplify the analysis, from now on, we take the Lagrangian to be $\mathcal{L}' = \mathcal{L}^2$; this corresponds to a reparametrization which leaves the length of the curve solving the Euler-Lagrange (EL) equations invariant [2,3].

Our goal is to minimize the time \mathcal{T} and thus obtain the time-optimal curve, or set of time-dependent controls. This optimal curve is the QAB. From variational calculus, the optimal path $\mathbf{x}_{\text{QAB}}(s)$ should satisfy $\delta \mathcal{T}[\mathbf{x}(s)]/\delta \mathbf{x}(s) = 0$, which gives rise to the EL equations $d\partial_{\dot{\mathbf{x}}} \mathcal{L}'[\dot{\mathbf{x}}, \mathbf{x}]/ds = \partial_{\mathbf{x}} \mathcal{L}'[\dot{\mathbf{x}}, \mathbf{x}]$.

Some remarks regarding the QAB are in order. (i) The total real evolution time T (for a given fidelity F) is not necessarily the same as \mathcal{T} . The correct interpretation is this: after finding the optimal path $\mathbf{x}_{\text{QAB}}(s)$ we solve the Schrödinger equation $i v_{\text{ad}} \partial_s |\psi\rangle = H|\psi\rangle$ with H and v_{ad} computed along the optimal path, to find $|\psi[\mathbf{x}_{\text{QAB}}(t)]\rangle$. The actual adiabatic error is then $\delta(T) \equiv \sqrt{1 - F_{\text{QAB}}(T)^2}$, where $F_{\text{QAB}}(T) \equiv |\langle \Phi_0(T) | \psi[\mathbf{x}_{\text{QAB}}(T)] \rangle|$, for a given T . With this interpretation it is safe to take $\epsilon \equiv 1$ in Eq. (3). Thus, we use \mathcal{T} as a guiding principle to obtain optimal paths; the actual adiabatic time and error should be calculated independently, as per the prescription above. (ii) Eq. (1) and our corresponding choice of v_{ad} are not unique. They merely represent a convenient ansatz for our subsequent analysis, and it is quite possible that a better ansatz involving a different combination of $\|\partial_s H\|$ and Δ exists. For other combinations ($\|\partial_s^k H\|^m / \Delta^l$) compatible with the adiabatic theorem [11], the time-optimal approach of Eq. (2) still remains applicable. However, this optimization may not induce a corresponding Riemannian geometry. (iii) The presence of Δ in \mathcal{L} implies that in order to apply our method, one needs to either find the gap exactly (which could be as hard as solving the problem itself), or restrict the interpolation to forms for which an explicit functional form for the gap can be obtained (e.g., in exactly solvable or almost-exactly solvable models), or follow the

scheme suggested to translate a quantum circuit model computation to an AQC (by which an interpolating Hamiltonian with an easily calculable gap is derived) [6], or estimate the gap by means of other methods. (iv) The bottleneck of adiabatic algorithms is at the finite-size precursor of QPTs where the gap becomes small (and vanishes in the thermodynamic limit) [5]. However, due to the $\|\dot{x}^i \partial_i H\|$ factor in the numerator of \mathcal{L} , in principle, there is the possibility that one can (at least partially) suppress the vanishing gap and associated QPT [13]. The QAB will inherently seek to identify such criticality-suppressing control strategies (relative to the specific adiabatic condition we have adopted here), if they exist. (v) Modeling AQC usually necessitates a parametrization of the Hamiltonian. In general, though, this parametrization is not unique. For simplicity, consider the parametrization $H(\mathbf{x}) = \sum_i x^i \sigma_i$, where $\{\sigma_i\}_{i=1}^M$ are time-independent, noncommuting, linearly independent Hermitian operators, chosen in accordance with the underlying structure of the optimization or physical problem in question. For example, in a multiqubit system, $\{\sigma_i\}$ could represent (two-) local interactions in the form of the tensor product of Pauli matrices. It can be shown that in these ‘‘interaction coordinates,’’ the EL equations read:

$$\ddot{x}^k + \Gamma_{ij}^k(\mathbf{x}) \dot{x}^i \dot{x}^j = 0, \quad (4)$$

where

$$\Gamma_{ij}^k = 2(C_{ij} C^{kl} \partial_l \Delta - \delta_i^k \partial_j \Delta - \delta_j^k \partial_i \Delta) / \Delta, \quad (5)$$

$C_{ij} \equiv (\mathbf{C})_{ij} = \text{Tr}[\sigma_i \sigma_j]$, and $C^{ij} = (\mathbf{C}^{-1})_{ij}$.

Geometrization of AQC.—Motivated by the existence of a differential-geometric description for circuit optimization [2], and by the resemblance of Eq. (4) to a geodesic equation [3], we reformulate QAB in a Riemannian geometric language, showing that the problem of finding the QAB can be viewed as belonging to geometric control theory [14]. The transition from the EL equations to a geodesic equation is possible when one can write $\mathcal{L}'[\dot{\mathbf{x}}, \mathbf{x}] = g_{ij}(\mathbf{x}) \dot{x}^i \dot{x}^j$, where \mathbf{g} (with matrix elements g_{ij}) is a differentiable and invertible matrix [3]. From the definition of \mathcal{L} for the QAB, we then obtain

$$g_{ij}(\mathbf{x}) = \text{Tr}[\partial_i H(\mathbf{x}) \partial_j H(\mathbf{x})] / \Delta^4(\mathbf{x}), \quad (6)$$

which is the sought-after metric tensor. In interaction coordinates, for example, $\mathbf{g}(\mathbf{x}) = \mathbf{C} / \Delta^4(\mathbf{x})$.

In this framework, then, the QAB is equivalent to the geodesic over $(\mathcal{M}, \mathbf{g})$, and Eq. (4) is the geodesic equation, in which $\Gamma_{ij}^k = \frac{1}{2} g^{kl} (\partial_j g_{li} + \partial_i g_{lj} - \partial_l g_{ij})$ are the connection coefficients [where $g^{ij} \equiv (\mathbf{g}^{-1})_{ij}$]. Since $g_{ij} \propto \Delta^{-4}$ (if the numerator does not contribute a power of Δ) we find $\Gamma \sim g^{-1} \partial g \sim \Delta^{-1} \partial \Delta$. Using standard expressions [3], one can calculate the Riemann curvature tensor \mathbf{R} from the connection coefficients and the metric tensor, yielding $\mathbf{R} \sim \partial^2 g + g \Gamma^2 \sim \Delta^{-6}$.

Examples.—We consider the following two-dimensional (2D) interpolating Hamiltonian:

$$H(x^1(s), x^2(s)) = x^1(s)P_{\mathbf{a}}^\perp + x^2(s)P_{\mathbf{b}}^\perp, \quad (7)$$

where $P_{\mathbf{a}}^\perp = \mathbb{1} - |\mathbf{a}\rangle\langle\mathbf{a}|$ for the normalized vector $|\mathbf{a}\rangle \in \mathcal{H}$ with $\dim(\mathcal{H}) = N$ (similarly for $P_{\mathbf{b}}^\perp$), $\alpha_0 \equiv \langle\mathbf{a}|\mathbf{b}\rangle$ is a known function of N alone, and $x^1(0) = x^2(1) = 1$; $x^1(1) = x^2(0) = 0$. It is evident that $|\mathbf{a}\rangle$ ($|\mathbf{b}\rangle$) is the ground state at $s = 0$ ($s = 1$). We can always find $|\mathbf{a}^\perp\rangle$ such that $|\mathbf{b}\rangle = \alpha_0|\mathbf{a}\rangle + \alpha_1|\mathbf{a}^\perp\rangle$, where $\langle\mathbf{a}|\mathbf{a}^\perp\rangle = 0$, and $\alpha_1 = \langle\mathbf{a}^\perp|\mathbf{b}\rangle$. Completing $\{|\mathbf{a}\rangle, |\mathbf{a}^\perp\rangle\}$ to a basis for \mathcal{H} we can easily diagonalize the Hamiltonian (7). While the general 2D problem requires a numerical solution, we find that if we impose a one-dimensional (1D) constraint, i.e., $x(s) \equiv x^2(s) = 1 - x^1(s)$, then an analytical solution is possible:

$$x_{\text{QAB}}(s) = \frac{1}{2} - \frac{|\alpha_0|}{2\sqrt{1-|\alpha_0|^2}} \tan[(1-2s)\arccos|\alpha_0|]. \quad (8)$$

We now consider two illustrative problems which are special cases of the Hamiltonian (7).

Quantum search.—As a first illustration we revisit Grover’s unstructured search problem, which involves finding a marked object among N objects by repeated oracle queries [1,15]. Grover’s quantum circuit model solution uses $O(\sqrt{N})$ queries, which is provably optimal, and a quadratic improvement over the best possible classical strategy. This problem was successfully recast in the AQC setting by Roland and Cerf (RC) [12], who considered the 1D version of (7) with $x(s) \equiv x^2(s) = 1 - x^1(s)$, $|\mathbf{a}\rangle = \sum_{k=0}^{N-1} |k\rangle/\sqrt{N}$ (equal superposition), $|\mathbf{b}\rangle = |m\rangle$, and the fixed index $m \in \{0, \dots, N-1\}$ being the “marked item.” Thus $\alpha_0 = 1/\sqrt{N}$, with $N = 2^n$ the dimension of the Hilbert space of n qubits. It turns out that the optimal 1D solution (8) coincides precisely with the solution found by RC, who proved its optimality [in the sense of $O(\sqrt{N})$ scaling for a fixed error] without the use of variational optimization. We now extend the analysis by considering 2D and 4D parametrizations, which corresponds to finding optimal curves on 2D and 4D manifolds, respectively. The 2D case is given by Eq. (7) and the discussion that follows it, with $|\mathbf{a}\rangle$ and $|\mathbf{b}\rangle$ as above. In the 4D case, we first consider a general 2×2 Hamiltonian $H(\{x^i\}) = \frac{1}{\sqrt{2}}(x^1\mathbb{1} +$

$x^2\sigma_x + x^3\sigma_y + x^4\sigma_z$), and solve the corresponding geodesic (or QAB) differential equations. Next we recall that Grover’s search is effectively a 2D problem (in the $\{|\mathbf{a}\rangle, |\mathbf{m}\rangle\}$ basis). This enables us to use the 4D setting for finding a Groverian geodesic path, with the proper boundary conditions corresponding to $|\mathbf{a}\rangle = \sqrt{(N-1)/N}|0\rangle + 1/\sqrt{N}|1\rangle$ and, for example, $|\mathbf{m}\rangle = |1\rangle$. It appears, from the solutions of the EL equations, that the path for these boundary conditions is effectively 2D. However, it still offers a relative advantage even over the 2D path of Eq. (7)—Fig. 1 (middle).

The 1D RC analysis employed the local adiabatic condition (1) to recover the optimal scaling $T_{\text{opt}} \propto \sqrt{N}$, for $N \gg 1$. This might suggest that there is no room for further improvement, but we recall that in the AQC setting the fidelity is 1 only in the limit $T \rightarrow \infty$. Thus we compare the error $\delta(T)$ for the RC interpolation to the error obtained from the optimal 2D interpolation. The result for $n = 6$ qubits is shown in Fig. 1 (left); results for other values of n are qualitatively similar, though the advantage of the optimal interpolation shrinks as n grows. The optimal 2D interpolation results in a smaller error for most values of T , a tendency that increases as T grows. Conversely, for most values of the error δ the 2D QAB requires a smaller time T than the RC curve. The middle panel shows the further improvement resulting from the 4D interpolation. These results provide a rather striking demonstration of the power of our formalism, as due to its highly optimized nature, the Grover example is one where hardly any improvement was to be expected.

Figure 1 (right) depicts the RC and 2D optimal curves over the curvature R_{1212} surface. Clearly, the optimal curve follows a path of lower curvature. This is confirmed in Fig. 2 (left), for different values of n . In spite of its improved performance, there is less entanglement along the 2D optimal path than along the RC path [Fig. 2 (right)], so that more entanglement does not always translate into higher algorithmic efficiency. We have verified (not shown) that the same picture emerges in terms of the entanglement entropy (or block entanglement) [16]. The explanation for this lower entanglement along the QAB is that it has a larger instantaneous gap than the RC path [Fig. 2 (right)]. Indeed, it has been shown that for Grover’s

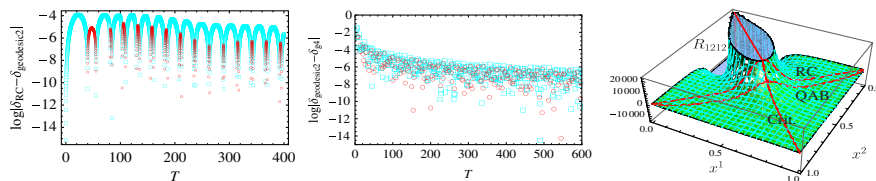


FIG. 1 (color online). Left: Final-time error $\delta(T)$ for the RC and 2D geodesic paths for the Grover search problem, for $n = 6$ qubits. Squares (cyan) indicate where the 2D geodesic path outperforms the RC path ($\delta_{\text{geodesic}} \leq \delta_{\text{RC}}$); circles (red) correspond to the opposite case. Oscillations are due to $\delta(T)$ itself being highly oscillatory, with an envelope $\propto 1/T$. Middle: $\delta(T)$ for the 2D and 4D geodesic paths, for $n = 1$. Cyan squares (red circles) indicate where the 4D (2D) geodesic path results in a smaller error. Right: Component $R_{1212}(x^1, x^2)$ of the curvature tensor for $n = 3$. The curves on the curvature surface show the critical line (vanishing gap as $n \rightarrow \infty$), the RC interpolation, and the 2D geodesic (QAB). Here R_{1212} is the only independent component of the curvature tensor.

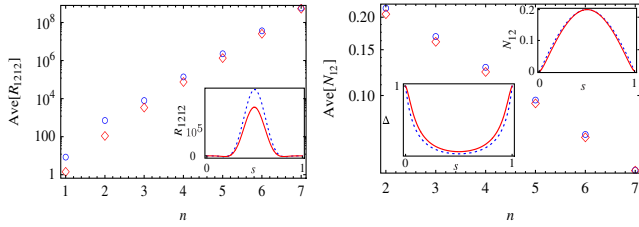


FIG. 2 (color online). Red diamonds or solid line (blue circles or dashed line) represent the 2D QAB (RC) path. Left: Average curvature component R_{1212} vs n . Inset: instantaneous curvature for $n = 4$. Results for other values of n are qualitatively similar. Right: Same for negativity N_{12} [21]—between qubits 1 and 2. Inset: instantaneous gap (lower left) and negativity (upper right) for $n = 4$. Here, $\text{Ave}_\gamma[X] \equiv \int_\gamma X[\mathbf{x}(s)]ds / \int_\gamma ds$ for given path γ ; $X \in \{N_{12}, R_{1212}\}$ and $\gamma \in \{\text{RC}, \text{QAB}\}$.

algorithm the entanglement entropy is small away from the finite-size precursor of the first-order QPT, but peaks near the critical point [5], and we have verified the same for the 2D QAB. Finally, the reason that QAB follows a path with larger gap is that this is consistent with higher adiabaticity. By our previous scaling result $\mathbf{R} \sim \Delta^{-6}$, it is also consistent with lower curvature.

Linear equations.—Solving linear equations of the type $\mathbf{A}\mathbf{y} = \mathbf{a}$, where \mathbf{A} is a given (Hermitian) $N \times N$ matrix and \mathbf{a} is a given vector, is a common problem. Recently a quantum algorithm was proposed in the circuit model that can obtain \mathbf{y} for well-conditioned, sparse matrices in a time scaling as $\text{polylog}(N)$ [17]. Here we consider the problem of finding $\mathbf{y} = \mathbf{A}^{-1}\mathbf{a}$ as one of oracular adiabatic state generation [18]. To do so we let $|\mathbf{b}\rangle = \mathbf{A}^{-1}|\mathbf{a}\rangle / \|\mathbf{A}^{-1}|\mathbf{a}\rangle\|$. The formulation given above for the Hamiltonian (7) then applies. For concreteness we let $|\mathbf{a}\rangle = (1, \dots, 1)^T / \sqrt{N}$ and take \mathbf{A} to be an $N \times N$ Toeplitz matrix whose first row and column are successive natural numbers, starting from 1. Toeplitz matrices have important applications in signal processing, and are not sparse. We then find numerically that $\alpha_0 = \sqrt{2/N}$ and hence can deduce immediately—by analogy to the Grover case, where $\alpha_0 = \sqrt{1/N}$ —that the optimal 1D interpolation will give rise to a run-time T scaling as $O(\sqrt{N})$ for a fixed error. Moreover, 2D and 4D interpolations will further improve the error at fixed run time. It is interesting to note that the most efficient known classical algorithm for inverting an $N \times N$ Toeplitz matrix requires $O(N \log^2 N)$ steps [19], though a direct comparison is not possible due to our oracular setting.

Conclusion and outlook.—We have presented a time-optimal, differential-geometric framework for AQC, and discussed its implications for the optimal design of adiabatic algorithms. The power of this new framework was illustrated via an example showing how the performance of an adiabatic algorithm can be improved by increasing the dimension of the control parameter space, and how geo-

metrization sheds light on the role of entanglement and control manifold curvature in this enhanced performance. The method presented here is general and can in principle be used to optimize any adiabatic quantum algorithm for which the gap (or estimate thereof) is known. An important next step is to incorporate decoherence-mitigation strategies [20].

Supported by the NSF under Grants No. CCF-726439, No. PHY-802678, No. PHY-803304, and No. PHY-0803371, and by NSERC and MRI.

- [1] M. A. Nielsen and I. L. Chuang, *Quantum Computation and Quantum Information* (Cambridge University Press, Cambridge, U.K., 2000).
- [2] M. A. Nielsen *et al.*, *Science* **311**, 1133 (2006); M. A. Nielsen, *Quantum Inf. Comput.* **6**, 213 (2006).
- [3] M. Nakahara, *Geometry, Topology and Physics* (Adam Hilger, New York, 1990).
- [4] E. Farhi *et al.*, arXiv:quant-ph/0001106; E. Farhi *et al.*, *Science* **292**, 472 (2001).
- [5] J. I. Latorre and R. Orús, *Phys. Rev. A* **69**, 062302 (2004); R. Schützhold and G. Schaller, *Phys. Rev. A* **74**, 060304 (2006).
- [6] D. Aharonov *et al.*, *SIAM J. Comput.* **37**, 166 (2007); A. Mizel, D. A. Lidar, and M. Mitchell, *Phys. Rev. Lett.* **99**, 070502 (2007).
- [7] This QAB is essentially different from the brachistochrone derived from nonadiabatically constrained dynamics, as in A. Carlini *et al.*, *Phys. Rev. Lett.* **96**, 060503 (2006).
- [8] A. Messiah, *Quantum Mechanics* (Dover Publication, New York, 1999).
- [9] K.-P. Marzlin and B. C. Sanders, *Phys. Rev. Lett.* **93**, 160408 (2004); D. M. Tong *et al.*, *Phys. Rev. Lett.* **98**, 150402 (2007); M. H. S. Amin, *Phys. Rev. Lett.* **102**, 220401 (2009).
- [10] J. Du *et al.*, *Phys. Rev. Lett.* **101**, 060403 (2008).
- [11] S. Jansen, M. -B. Ruskai, and R. Seiler, *J. Math. Phys.* (N.Y.) **48**, 102111 (2007); D. A. Lidar, A. T. Rezakhani, and A. Hamma, arXiv:0808.2697.
- [12] J. Roland and N. J. Cerf, *Phys. Rev. A* **65**, 042308 (2002).
- [13] G. Schaller, *Phys. Rev. A* **78**, 032328 (2008); M. B. Hastings, *J. Stat. Mech.* (2008) L01001.
- [14] V. Jurdjevic, *Geometric Control Theory* (Cambridge University Press, Cambridge, U.K., 1996).
- [15] L. K. Grover, *Phys. Rev. Lett.* **79**, 4709 (1997).
- [16] G. Vidal *et al.*, *Phys. Rev. Lett.* **90**, 227902 (2003).
- [17] A. Harrow, A. Hassidim, and S. Lloyd, arXiv:0811.3171.
- [18] D. Aharonov and A. Ta-Shma, *SIAM J. Comput.* **37**, 47 (2007).
- [19] G. S. Ammar and W. B. Gragg, *SIAM J. Matrix Anal. Appl.* **9**, 61 (1988).
- [20] S. P. Jordan, E. Farhi, and P. W. Shor, *Phys. Rev. A* **74**, 052322 (2006); D. A. Lidar, *Phys. Rev. Lett.* **100**, 160506 (2008).
- [21] G. Vidal and R. F. Werner, *Phys. Rev. A* **65**, 032314 (2002).